JOURNAL OF NANO- AND ELECTRONIC PHYSICS
Vol. **12** No 2, 02001(4pp) (2020)

ЖУРНАЛ НАНО- ТА ЕЛЕКТРОННОЇ ФІЗИКИ
Том **12** № 2, 02001(4cc) (2020)

Analytical Study of Graphene as a Novel Piezoresistive Material for MEMS Pressure Sensor Application

Samridhi[1], Mayuri Sharma[1], Kulwant Singh[2], Shalendra Kumar[3], P.A. Alvi[1,*]

[1] *Department of Physics, Banasthali Vidyapith-304022 Rajasthan, India*
[2] *Department of Electronics and Communication Engineering, Manipal University Jaipur, Jaipur 303007 Rajasthan, India*
[3] *Department of Physics, College of Science, King Faisal University, Hofuf, Al-Ahsa 31982 Saudi Arabia*

(Received 15 February 2020; revised manuscript received 12 April 2020; published online 25 April 2020)

The one-atom thick layer of carbon has been investigated with its unique exclusive property such as high thermal conductivity due to the high velocity of electron and exceptional electrical conductivity as well as mechanical strength. Due to its extraordinary properties; graphene put back many conventional materials to due smart, sensitive applications. As graphene has no band gap (*Eg* ~0 eV) but there is one method to induce a band gap by applying strain and each specific strain direction will create a unique band gap structure, in return it give signals which can be sensed by the device. The device can be operated either optically or electrically at different pressure levels up to Tera Pascal range thereby providing designers and engineers with a versatile sensing solution. To fabricate MEMS sensor based on a single layer of graphene, the piezoresistive pressure is becoming the most devastating problem up to nanoscale without damaging and high quality, defect free graphene. In this paper, we discussed the issues and cost effective solutions to integrate MEMS/NEMS pressure sensor device. We also compared the sensor performance with traditional piezoresistive materials.

Keywords: Graphene, Piezoresistive, Sensors, MEMS.

DOI: 10.21272/jnep.12(2).02001 PACS numbers: 05.50. + q, 81.40.Vw, 81.90. + c

1. INTRODUCTION

In 2004, graphene was discovered experimentally, by the Manchester group led by A. Geim, and K.S. Novoselov [1], who earned Nobel Prize in 2010 on behalf of the "groundbreaking experiments regarding the two-dimensional material graphene". Graphene has shown lots of extraordinary properties, which make it capable to be used in electronic devices. An electronic quality of material is generally characterised by the mobility of electron and graphene shows high electronic mobility equal to 200,000 cm^2/Vs for graphene sheet [2] and outstanding mechanical property, making it a perfect material for MEMS applications, together with sensing and signal processing. A theoretical simulation of graphene was carried out in order to calculate its *k*-space energy band structure with variable c-c bond length and c-c transfer energy resulting into its unique properties [3]. Graphene has no band gap (E_g ~ 0 eV), as shown in Fig. 1(b), but there is one method to induce a band gap by applying strain and each specific strain direction will create a unique band gap structure. Tight-binding model [4] has been used to measure the deflection of monolayer graphene and effects on the band structure in suspended graphene devices.

2. GRAPHENE ANALYSIS

In order to calculate the surface charge density and density of states, a PBE-GGA (Perdew-Burke-Ernzerhof generalized-gradient-approximation) is utilized within the frame work of wein2k code. The total and partial densities of states (TDOS/PDOS) are shown in Fig. 2a. At 8 eV, a peak (of value ~ 2.4 states/eV) of red color is observed showing total density of states due to sp^2 hybridization of C-atom. This is mainly due to C-2*p* orbital which means that at this particular energy, many states are available for occupation. In Fig. 2(b), investigated charge density of monolayer graphene is shown by contour plot which tells the nature of bonding between C-C atoms. The charge density contour lines show the strong covalent bonding between C-C atoms.

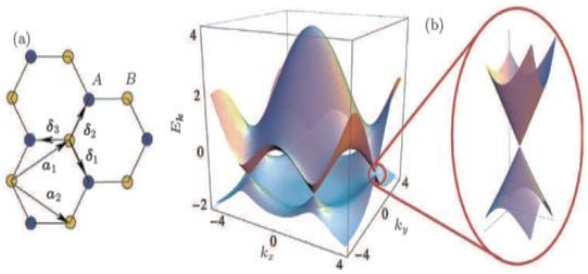

Fig. 1 – Graphene: Lattice structure (a); Band structure in *k*-space (b)

Graphene can be synthesized with the array of techniques. Mechanical exfoliation of graphene was the first method to attain monolayer graphene sheet. Though, this technique has no control over many layers. A chemical vapor deposition was the second most promising technique for the synthesis of good quality, graphene sheets.

3. ROLE OF GRAPHENE IN MEMS PRESSURE SENSORS

Graphene is an ideal two-dimensional (2*D*) material

* drpaalvi@gmail.com

therefore; it has an advantage in scalable device fabrication via top-down approaches, which is well-suited with the existing MEMS technology. As compared with other strain sensors, graphene based devices are ultra-thin transparent and these are easily obtained and utilized commercially. Its principle is based on the fact that when pressure is applied on it, a change in resistance can be achieved. Due to remarkable properties of graphene, it is leading to a significant elongation in strain sensors. When strain is applied there is shift in its electronic band structure and relative change observed in electrical properties, therefore notable electromechanical coupling is observed.

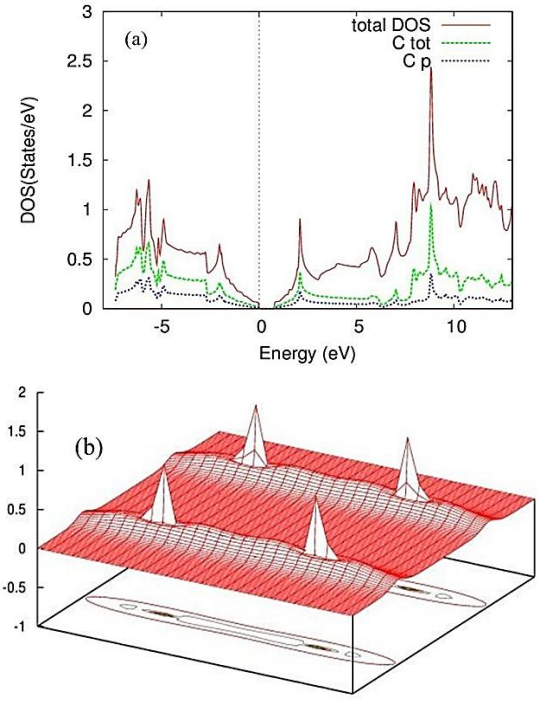

Fig. 2 – Plot of Graphene DOS (a) and charge distribution on graphene monolayer (b)

In the Table 1, various parameters of different pressure sensors utilizing different materials are compared and discussed.

3.1 DESIGN CONSIDERATION OF GRAPHENE BASED SENSOR

Fig. 3 shows the schematic design of graphene based pressure sensor. The substrate of pressure sensor is made from single-crystal Si material with dimensions of 4 mm × 4 mm. The dimensions of diaphragm have been taken as 2 mm×2 mm; while thickness is ~ 50 μm.

The piezoresistors are made of graphene having length of 400 μm and resistor line width is 10 μm, the contact pads and metal lines are made of gold having 200 μm × 200 μm dimension. The shape and location of piezoresistors are chosen is such a way, that each piezoresistor could contribute maximum influence on sensitivity.

The designed sensor has been etched to get maximum stress. The TMAH (Tetra-methyl-ammonium hydroxide) etching process has been carried out such that its edges are fixed and central part is flexible. The sensor has been subjected to external pressure within in the range of 10-100 psi.

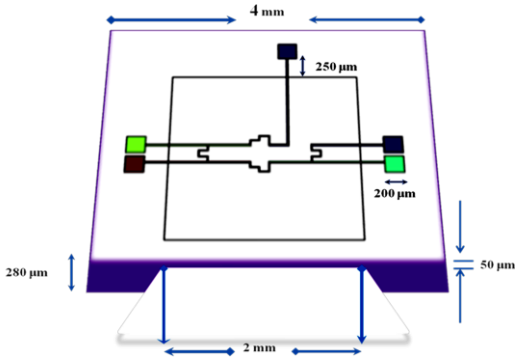

Fig. 3 – Lateral View and layout of designed graphene based pressure sensor

Table 1 – Comparison of various Sensor technologies with respect to reported sensitivities, gauge factor, pressure, young's modulus and response time.

Material	Type	Gauge Factor	Young's Modulus (kPa)	Sensitivity (without TPR) (kPa^{-1})	Sensitivity (with TPR) (kPa^{-1})	Pressure Applied (kPa)	Response time (ms)
SWCNT [7]	Piezoresistive	2.9×10^3	~ 1×10^9	27.5 %/nm	_	~10 [14]	70 [13]
GO [8]	Piezoresitive	_	2.07×10^8	0.96	_	0 ~ 50	0.4
SILICON [9]	Capacitance	_	17×10^7	9.3895×10^{-12} F	1.105×10^{-11} F	0.02	_
Graphene [9]	Capacitance	_	≥ 1×10^9	1.18×10^{-12} F	1.18×10^{-12} F	0.02	_
ZnO [10]	Piezoelectric	1.25×10^3	4×10^7	_	_	_	10
ZnO (array) [11]	Piezophotonic	_	4×10^7	12.88×10^6	_	_	90
Graphene [12]	Piezoresisitve	1.8×10^4	≥ 1×10^9	_	_	_	600 [14]

4. RESULT AND DISCUSSION

A Von-Mises stress distribution has been shown in square diaphragm under applied pressure range of 10-100 psi, as illustrated in Fig. 4. The simulation profile shows a high stress region along the edges of diaphragm. The piezoresistors must be positioned in these high stress areas to experience the maximum stress in order to obtain better piezoresistance. The early outcomes of our research work based on polysilicon MEMS pressure sensor have been shown in literature [15-18].

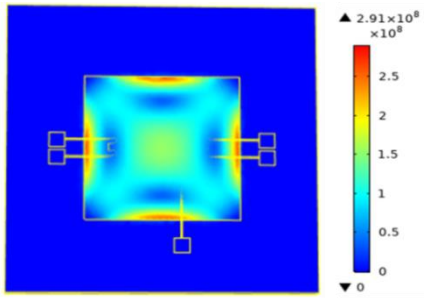

Fig. 4 – Von-Mises stress profile of a square diaphragm showing high stress regions

On applying the pressure the diaphragm tends to deform and induces stress within the material.

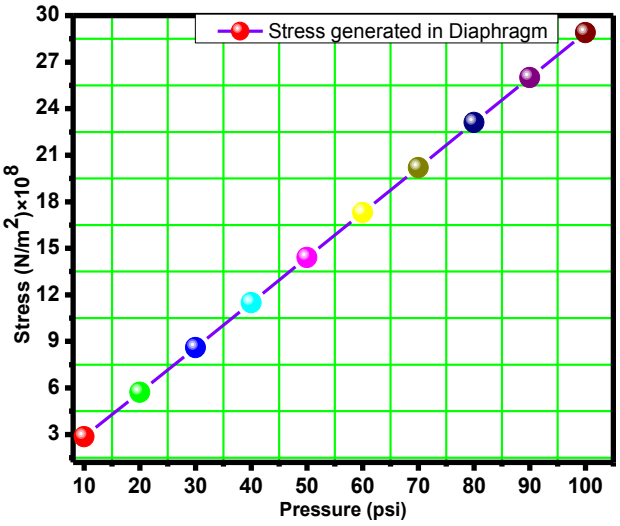

Fig. 5 – Stress generated vs pressure in a square diaphragm

Through FEM analysis, the location of maximum *V*on Mises stress has been optimized, Fig. 5 shows the maximum stress induced in the diaphragm is ~ 29.1×10^8 N/m^2.

Fig. 6 shows the effect of pressure on four piezoresistors revealing that oppositely placed resistors exhibit's the same stress of order of ($13.2\text{-}14.7 \times 10^8$ N/m^2) for resistors R_1 and R_3. While for R_2 and R_4 ($3.7\text{-}4.17 \times 10^8$ N/m^2) has been optimized.

The edges of the substrate are fixed and central part is flexible, the pressure causes the central part to displace up to some extent. Thus, Fig. 7 shows the simulation profile of the designed pressure sensor and Fig. 8 shows the displacement plot of pressure sensor, showing the maximum displacement of 7.2 μm.

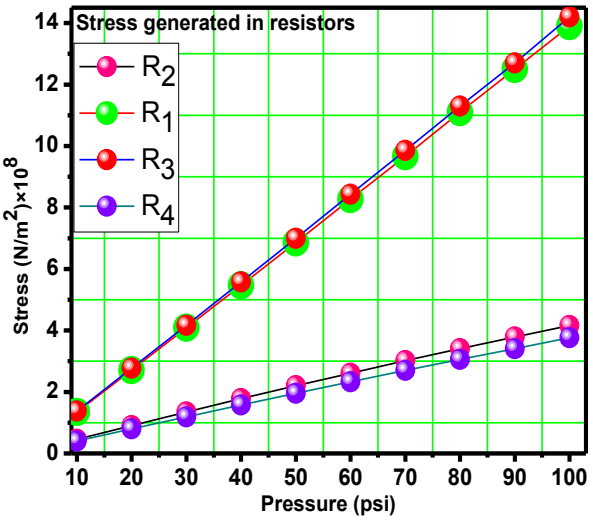

Fig. 6 – Stress induced in four piezoresistors

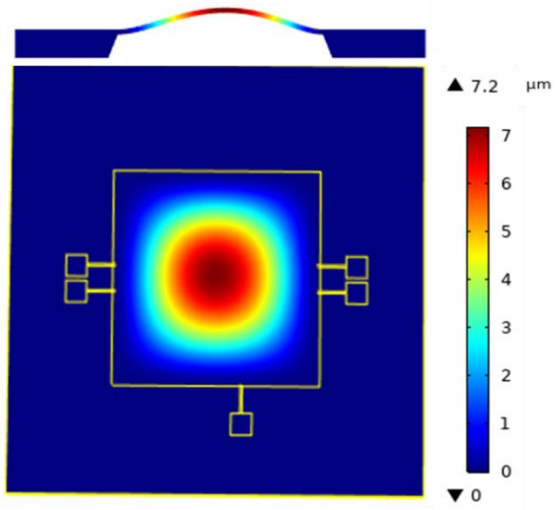

Fig. 7 – Simulation profile of a displacement in square diaphragm

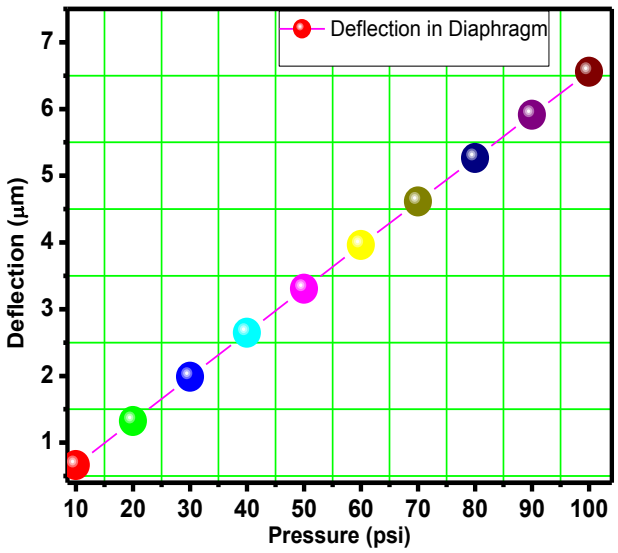

Fig. 8 – Displacement plot of square diaphragm

CONCLUSION

In this paper, an analytical study in terms of its density of states and charge distribution of graphene is carried out in order to find its application in MEMS based pressure sensor. In the study, the results show the promising future of single layer graphene-based MEMS pressure sensor and their ability to become a serious competitor to other sensor technologies.

AKNOWLEDGEMENTS

Authors are grateful to Banasthali Vidyapith for providing research facilities under CURIE programme supported by the DST, Government of India, New-Delhi.

REFERENCES

1. G. Mukhopadhyay, H. Behera, arXiv preprint arXiv: **1306.0809** (2013).
2. K.I. Bolotin, K.J. Sikes, Z. Jiang, M. Klima, G. Fudenberg, J. Hone, H.L. Stormer, *Solid State Commun.* **146** No 9, 351 (2008).
3. P.A. Alvi, S.Z. Hashmi, S. Dalela, F. Rahman, *J. Nano-Electron. Phys.* **3** No 3, 42 (2011).
4. V.M. Pereira, A.C. Neto, N.M.R. Peres, *Phys. Rev. B* **80**, 045401 (2009).
5. P.A. Alvi, B.D. Lourembam, V.P. Deshwal, B.C. Joshi, J. Akhtar, *Sensor Rev.* **26** No 3, 179 (2006).
6. Kulwant Singh, R. Joyce, S. Varghese, J. Akhtar, *Sensor. Actuat. A* **223**, 151 (2015).
7. C. Stampfer, A. Jungen, R. Linderman, D. Obergfell, S. Roth, C. Hierold, *Nano Lett.* **6** No 7, 1449 (2006).
8. H. Tian, Y. Shu, X.F. Wang, M.A. Mohammad, Y. Yang, T.L. Ren, *2014 IEEE International Electron Devices Meeting*, 15 (2014).
9. V. Amith, Sushil, T. Vyasaraj, G. Hatti, V. Kumar, S. Kumar, V. Kumari, D.S. Kamble, *International Journal of Innovative Research in Science, Engineering and Technology* **5** No 5, 8407 (2016).
10. J. Zhou, Y. Gu, P. Fei, W. Mai, Y. Gao, R. Yang, G. Bao, Z.L. Wang, *Nano Lett.* **8** No 9, 3035 (2008).
11. C. Pan, L. Dong, G. Zhu, S. Niu, R. Yu, Q. Yang, Y. Liu, Z.L. Wang, *Nat. Photon.* **7** No 9, 752 (2013).
12. H. Hosseinzadegan, C. Todd, A. Lal, M. Pandey, M. Levendorf, J. Park, *2012 IEEE 25th International Conference on Microelectro Mechanical Systems (MEMS)*, 611 (2012).
13. J. Park, Y. Lee, S. Lim, Y. Lee, Y. Jung, H. Lim, H. Ko, *BioNanoScience* **4** No 4, 349 (2014).
14. A.D. Smith, K. Elgammal, F. Niklaus, A. Delin, A.C. Fischer, S. Vaziri, F. Forsberg, *Nanoscale* **7** No 45, 19099 (2015).
15. Samridhi, Meha Sharma, Kulwant Singh, P.A. Alvi, *AIP Conf. Ser.* **2100** No. 2, 020132 (2019).
16. Samridhi, Manish Kumar, Kulwant Singh, P.A. Alvi, *IOP Conf. Ser.: Mater. Sci. Eng.* **594**, 012045 (2019).
17. Samridhi, Manish Kumar, Kulwant Singh, *AIP Conf. Ser.* **2115** No 3, 030464 (2019).
18. Samridhi, Manish Kumar, Sachin Dhariwal, Kulwant Singh, P.A. Alvi, *Int. J. Modern Phys. B* **33** No 7, 1950040 (2019).